Published in final edited form as:

Mol Cell. 2018 August 16; 71(4): 592–605.e4. doi:10.1016/j.molcel.2018.06.036.

DUB3 promotes BET inhibitor resistance and cancer progression through deubiquitinating BRD4

Xin Jin[1,2], **Yuqian Yan**[2], **Dejie Wang**[2], **Donglin Ding**[2], **Tao Ma**[2], **Zhenqing Ye**[3], **Rafael Jimenez**[4], **Liguo Wang**[3], **Heshui Wu**[1,*], and **Haojie Huang**[2,5,6,7,*]

[1]Department of Pancreatic Surgery, Union Hospital, Tongji Medical College, Huazhong University of Science and Technology, Wuhan, 430022, China

[2]Department of Biochemistry and Molecular Biology, Mayo Clinic College of Medicine, Rochester, MN 55905, USA

[3]Division of Biomedical Statistics and Informatics, Mayo Clinic College of Medicine, Rochester, MN 55905, USA

[4]Department of Laboratory Medicine and Pathology, Mayo Clinic College of Medicine, Rochester, MN 55905, USA

[5]Department of Urology, Mayo Clinic College of Medicine, Rochester, MN 55905, USA

[6]Mayo Clinic Cancer Center, Mayo Clinic College of Medicine, Rochester, MN 55905, USA

SUMMARY

The bromodomain and extra-terminal domain (BET) protein BRD4 is emerging as a promising anticancer therapeutic target. However, resistance to BET inhibitors often occurs and it has been linked to aberrant degradation of BRD4 protein in cancer. Here, we demonstrate that the deubiquitinase DUB3 binds to BRD4 and promotes its deubiquitination and stabilization. Expression of DUB3 is transcriptionally repressed by the NCOR2-HDAC10 complex. The *NCOR2* gene is frequently deleted in castration-resistant prostate cancer patient specimens, and loss of NCOR2 induces elevation of DUB3 and BRD4 proteins in cancer cells. DUB3-proficient prostate cancer cells are resistant to BET inhibitor JQ1 in vitro and in mice, but this effect is diminished by the DUB3 inhibitory agents such as CDK4/6 inhibitor in a RB-independent manner. Our findings identify a previously unrecognized mechanism causing BRD4 upregulation and drug

[*]Corresponding authors: Haojie Huang (huang.haojie@mayo.edu); Heshui Wu (heshuiwu@hust.edu.cn).
[7]Lead Contact

SUPPLEMENTAL INFORMATION

Supplemental Information includes seven figures and one table.

AUTHOR CONTRIBUTIONS

H.H., H.W. and X.J. conceived the study. X.J, Y.Y., D.W., D.D. conducted all the experiments. T.M., Z.Y., L.W. performed bioinformatics analysis. R.J. conducted patient specimen evaluation and IHC scoring. X.J., H.W., and H.H. wrote the manuscript. All authors read and commented on the manuscript appropriately.

DECLARATION OF INTERESTS

The authors declare no conflict of interest.

resistance, suggesting DUB3 is a viable therapeutic target to overcome BET inhibitor resistance in cancer.

eTOC Blurb

Increased expression of BRD4 protein has been linked to BET inhibitor resistance. Jin et al. identify DUB3 as a deubiquitinase of BRD4 and demonstrate that aberrant expression of DUB3 confers BET inhibitor resistance in cancer cells by promoting BRD4 protein deubiquitination and stabilization, which can be overcome by CDK4/6 inhibitor.

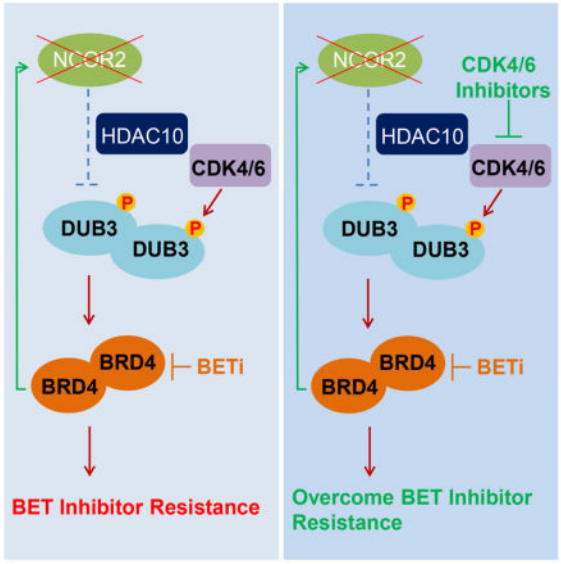

INTRODUCTION

BRD4 is a member of the bromodomain and extra terminal domain (BET) protein family. It plays a key role in gene transactivation by functioning as an epigenetic “reader” that facilitates recruitment of the positive transcription elongation factor P-TEFb through interaction with acetylated histones (Jang et al., 2005; Shi and Vakoc, 2014). Increasing evidence shows that BRD4 is involved in many biological processes, including cell cycle transition, cell proliferation, DNA damage response, autophagy, and memory formation (Floyd et al., 2013; Korb et al., 2015; Sakamaki et al., 2017; Wang and Filippakopoulos, 2015).

In addition to interacting with acetylated histones, BRD4 has also been shown to promote cancer progression by physically and/or functionally interacting with transcription factors in a cancer type-specific manner, such as MYC in multiple myeloma, androgen receptor (AR) in castration-resistant prostate cancer (CRPC), TWIST in breast cancer, and ERG in acute myeloid leukemia and prostate cancer (Asangani et al., 2014; Blee et al., 2016; Delmore et al., 2011; Roe et al., 2015; Shi et al., 2014). These findings highlight that BRD4 is a promising therapeutic target of cancer (Asangani et al., 2014; Delmore et al., 2011). Indeed, several small-molecule inhibitors specifically targeting the bromodomains of BET proteins, such as JQ1 and I-BET762, have been developed, and many of them are currently in clinical

trials for treatment of various human cancers (Filippakopoulos et al., 2010; Nicodeme et al., 2010). However, drug resistance often emerges and a number of underlying mechanisms have been identified in different cancer types (Fong et al., 2015; Rathert et al., 2015; Shu et al., 2016).

It has been shown recently that BRD4 is an ubiquitination and proteasome degradation target of the E3 ubiquitin ligase SPOP (Dai et al., 2017; Janouskova et al., 2017; Zhang et al., 2017). Further studies show that prostate cancer-associated SPOP mutations result in impaired degradation and upregulation of BRD4 protein, thereby conferring intrinsic resistance to bromodomain inhibitors (Dai et al., 2017; Janouskova et al., 2017; Zhang et al., 2017). Notably, endometrial cancer-associated SPOP mutations promote accelerated degradation and reduction of BRD4 proteins, thereby sensitizing cancer cells to BET inhibitors (Janouskova et al., 2017). These findings stress that aberrant elevation of BRD4 protein is a key determinant in development of BET inhibitor resistance.

By antagonizing E3 ubiquitin ligase-mediated protein polyubiquitination and proteasome degradation, deubiquitinases (DUBs) promote protein stabilization by removing the ubiquitin modifications from target proteins. DUB3 is a member of DUBs which is known to promote cell transformation and metastasis in multiple cancer types by specifically interacting with and stabilizing a few oncogenic proteins such as CDC5A and SNAIL (Liu et al., 2017; Pereg et al., 2010; Wu et al., 2017). Importantly, it has been shown recently in breast cancer cells that DUB3 can be phosphorylated by CYCLIN-dependent kinases 4 and 6 (CDK4/6) and this phosphorylation is essential for the deubiquitinase activity of DUB3 (Liu et al., 2017), highlighting that DUB3 is a druggable target for cancer therapy.

In this present study, we showed that expression of DUB3 is transcriptionally repressed by the NCOR2/HDAC10 transcription repression complex. Deletion of the *NCOR2* gene was detected in a subset of CRPC patients and loss of NCOR2 resulted in overexpression of DUB3 in prostate cancer cells. We identified BRD4 as *bona fide* substrate of DUB3 and showed that dysregulated DUB3 contributed to resistance to BET inhibitors by stabilizing BRD4 protein. Most importantly, we further demonstrated that DUB3 overexpression conferred resistance to BET inhibitor and this can be overcome by inhibition of DUB3 with the CDK4/6 inhibitor PD0332991 (palbociclib).

RESULTS

NCOR2 and HDAC10 transcriptionally repress expression of DUB3

It has been shown previously that treatment of pan class I/II HDAC inhibitors induces mRNA expression of *USP17L2* (also known as *DUB3* or *USP17*) in breast cancer cells (Borbely et al., 2015). Similarly, we found that treatment with the pan histone deacetylase inhibitor trichostatin A (TSA) increased DUB3 protein and mRNA expression in C4-2 prostate cancer cells (Figures 1A and 1B). To determine which member(s) in the class I/II HDAC subfamilies mediates the transcriptional repression of DUB3 expression, we performed an unbiased screen by knocking down all eleven class I/II HDACs individually by using small hairpin RNAs (shRNAs). We demonstrated that only knockdown of HDAC10 specifically resulted in a substantial increase in *DUB3* mRNA expression in C4-2 cells

(Figure 1C). HDAC10 knockdown also markedly increased DUB3 protein in C4-2 cells, and similar results were obtained in another prostate cancer cell line PC-3 (Figures 1D and 1E).

HDAC10 is a class II deacetylase that promotes gene transcription repression by forming a protein complex with nuclear receptor co-repressor (NCOR) proteins (Fischer et al., 2002). A study analyzing the co-expression of HDAC and NCOR genes in human gliomas shows that NCOR2 expression is clustered with HDAC10 and HDAC4 whereas NCOR1 is clustered with HDAC8 (Dali-Youcef et al., 2015). We therefore examined whether NCOR2 plays any role in regulating DUB3 expression. Reciprocal co-immunoprecipitation (co-IP) showed that endogenous HDAC10 and NCOR2 proteins interact with each other in C4-2 cells (Figures 1F and 1G). Similar to the effect of HDAC10 depletion (Figures 1D and 1E), knockdown of NCOR2 by two independent shRNAs increased DUB3 expression at both mRNA and protein level in C4-2 and PC-3 cells (Figures 1H and 1I). Chromatin Immunoprecipitation (ChIP) analyses demonstrated that both NCOR2 and HDAC10 occupied in the *DUB3* gene promoter in both C4-2 and PC-3 cells (Figures 1J and 1K), and their co-occupation in the *DUB3* gene promotor was further confirmed by ChIP-reChIP analyses (Figure 1L). Co-knockdown of NCOR2 and HDAC10 failed to further increase DUB3 expression at both protein and mRNA level in comparison to each knockdown alone (Figures 1M and 1N). These data suggest that NCOR2 and HDAC10 work in concert in the same complex to repress expression of DUB3 in prostate cancer cells (Figure 1O).

BRD4 represses DUB3 expression via transcriptional activation of NCOR2

It has been reported previously that treatment with the BRD4 inhibitor JQ1 induces rapid upregulation of *DUB3* at the mRNA level (Borbely et al., 2015). We sought to determine how DUB3 expression is regulated by BRD4. We analyzed existing BRD4 ChIP-seq data in our laboratory (Zhang et al., 2017) and noticed that there is no obvious detectable BRD4 binding peak in the promoter of *DUB3* gene even in BRD4 overexpressing cells (Figure S1A). These data suggest that BRD4 inhibition-induced downregulation of *DUB3* mRNA may be mediated through an indirect mechanism. Since we have identified NCOR2 and HDAC10 as upstream repressors of *DUB* mRNA expression (Figure 1), we asked whether BRD4 modulates DUB3 expression via regulating NCOR2 and/or HDAC10. Re-examination of BRD4 ChIP-seq data revealed a sharp BRD4 binding peak in the promoter of *NCOR2* but not *HDAC10* gene in BRD4 overexpressing C4-2 cells (Figures 2A and S1B). This result was further confirmed by ChIP-qPCR in both C4-2 and PC-3 cells (Figures 2B and 2C). Using a gain-of-function approach, we demonstrated that overexpression of BRD4 elevated NCOR2 expression but repressed DUB3 at both mRNA and protein levels in C4-2 cells (Figures 2D and 2E). In contrast, knockdown of BRD4 by two independent shRNAs decreased NCOR2 but increased DUB3 mRNA and protein expression in both C4-2 and PC-3 cells (Figures 2F and 2G). Most importantly, we demonstrated that both BRD4 knockdown and overexpression-induced upregulation and downregulation of DUB3, respectively were completely abolished by NCOR2 co-knockdown in C4-2 cells (Figures 2H and 2I). In a dose- and time-dependent manner the BRD4 inhibitor JQ1 decreased NCOR2 protein and mRNA expression in C4-2 cells and the effect of JQ1 on DUB3 protein and mRNA expression was opposite (Figures 2J–2M). It is worth noting that JQ1 treatment only increased BRD4 protein level, but not mRNA level (Figures 2J–2M), which is consistent

with previous reports in various cell types (Asangani et al., 2014; Lu et al., 2015; Zhang et al., 2017). Taken together, these data indicate that BRD4 induces downregulation of DUB3 through upregulation of NCOR2, which acts as a repressor of DUB3 transcription (Figure 2N).

DUB3 promotes deubiquitination of BRD4 protein

Upon examining the effect of JQ1 on DUB3 expression, we found that JQ1 induced upregulation of DUB3 at both mRNA and protein levels, but only upregulated BRD4 protein level without affecting its mRNA expression (Figure 2J–2M). Based upon these data, we hypothesized that DUB3 functions as a DUB that stabilizes BRD4 protein via deubiquitinating BRD4. To test this hypothesis, we co-expressed DUB3 with BRD4 in 293T cells and found that DUB3 increased BRD4 protein expression in a dose-dependent manner (Figure 3A). In contrast, knockdown of DUB3 by two independent shRNAs decreased the level of endogenous BRD4 proteins, but had no overt effect on *BRD4* mRNA expression in both PC-3 and DU145 cells (Figures 3B and S2A). Similar results were observed in broader cancer cell lines, including two more prostate cancer cell lines, two pancreatic cancer cell lines, and three breast cancer cell lines (Figures S2B–S2D). We further demonstrated that downregulation of BRD4 proteins caused by DUB3 knockdown was reversed by treatment of cells with the proteasome inhibitor MG132 (Figure 3C). Overexpression of HA-DUB3 WT, but not the deubiquitinase activity-deficient mutant C89S (Wu et al., 2017) increased the level of ectopically expressed Flag-BRD4 protein in a dose-dependent manner in PC-3 cells (Figure 3D). In agreement with these findings, knockdown of DUB3 shortened BRD4 protein half-life and dramatically increased endogenous BRD4 ubiquitination in PC-3 cells (Figures 3E and 3F). In contrast, overexpression of HA-DUB3-WT prolonged the half-life of ectopically expressed Flag-BRD4 protein (Figure 3G). Forced expression of DUB3-WT, but not the catalytically inactive mutant C89S (CS) (Liu et al., 2017) diminished the ubiquitination level of BRD4 in PC-3 cells (Figure 3H). We also examined whether the BRD4 protein level is regulated by other DUBs such as a number of cancer-relevant DUBs including USP7, USP10, USP13, USP15, USP28, USP49 (Deng et al., 2016; Turnbull et al., 2017; Wu et al., 2013; Zhang et al., 2013). We demonstrated that different from DUB3, none of these DUBs either interacted with BRD4 or affected BRD4 protein level in 293T and DU145 cells, respectively (Figures S3A and S3B). Thus, we identify DUB3 as a deubiquitinase that specifically promotes deubiquitination of BRD4 in prostate cancer cells. Our data suggest this regulatory mechanism may also exist in other cancer types such as breast and pancreatic cancer.

It has been reported recently that SPOP is an E3 ubiquitin ligase that promotes ubiquitination and proteasome degradation of BRD4 in prostate cancer cells (Dai et al., 2017; Janouskova et al., 2017; Zhang et al., 2017). We were interested to determine whether DUB3 influences SPOP-mediated ubiquitination and degradation of BRD4. As expected, expression of SPOP markedly decreased the protein level of ectopically expressed BRD4 in PC-3 cells (Figure 3I). However, this effect of SPOP was largely abolished by expression of DUB3-WT, but not by the C89S mutant (Figure 3I). Conversely, knockdown of DUB3 largely reduced the level of BRD4 protein in PC-3 cells (Figure 3J), although SPOP knockdown failed to completely reverse DUB3 knockdown-induced decrease of BRD4

protein levels (Figure 3J). Moreover, SPOP-mediated polyubiquitination of BRD4 was largely diminished by co-expression of DUB3 WT, but not the C89S mutant (Figure 3K). These data indicate that DUB3 stabilizes BRD4 by promoting BRD4 deubiquitination and SPOP-mediated ubiquitination of BRD4 can be offset by DUB3 (Figure 3L).

DUB3 specifically interacts with BRD4 in cells

To further investigate the relationship between DUB3 and BRD4, we performed reciprocal co-immunoprecipitation (co-IP) assays and demonstrated that ectopically expressed Flag-BRD4 interacted with ectopically expressed HA-DUB3 in 293T cells (Figures 4A and 4B). Interaction between endogenous BRD4 and DUB3 proteins was detected in PC-3 cells (Figures 4C and 4D). To define which region(s) in DUB3 interact with BRD4, we generated GST-DUB3 recombinant proteins as reported previously (Wu et al., 2017) (Figure 4E). GST pull-down assays indicated that the N-terminal fragment (aa 1-398) of DUB3, but not the C-terminal fragment or GST alone, bound specifically with BRD4 (Figure 4F). To determine which region(s) in BRD4 are involved in DUB3 binding, we constructed BRD4 deletion constructs as reported previously (Shi et al., 2014) (Figure 4G) and co-expressed them with DUB3 in 293T cells. Co-IP assays revealed that the C-terminal end of BRD4 containing amino acids (aa) 1047-1362 interacted with DUB3 (Figure 4H). Given that the C-terminal region in three ubiquitously expressed BET proteins including BRD2, BRD3, and BRD4 is very much diversified and only BRD4 contains the C-terminal motif (CTM) (Figure S4A), we sought to investigate whether the interaction between BRD4 and DUB3 is specific. Co-IP assays revealed that while DUB3 bound to BRD4, it did not bind to BRD2 and BRD3 in PC-3 cells (Figure 4D). We further demonstrated that BRD4-DUB3 interaction is mediated through the CTM motif in BRD4 (Figure 4I). Accordingly, we demonstrated that overexpression of DUB3 increased the level of ectopically expressed full-length BRD4 protein in a dose-dependent manner, but has no effect on BRD4 CTM mutant, BRD2 or BRD3 in PC-3 cells (Figures 4J, S4B and S4C). Furthermore, knockdown of DUB3 also failed to affect the expression of endogenous BRD2 and BRD3 proteins in PC-3 cells (Figure S4D). These data indicate that DUB3 specifically interacts with and modulates BRD4 expression at the protein level.

NCOR2 regulates DUB3 and BRD4 expression and its expression inversely correlates with DUB3 and BRD4 protein levels in prostate cancer specimens

It has been reported previously that BRD4 protein is upregulated in CRPC patients (Urbanucci et al., 2017). NCOR2 was found genomically deleted in a subset of CRPC patients (Robinson et al., 2015) (Figure S5A) and NCOR2 was more frequently deleted or mutated in metastatic prostate cancers compared to primary lesions (Cancer Genome Atlas Research, 2015). Intriguingly, meta-analysis showed that DUB3 mRNA level was significantly upregulated in CRPC patient samples compared to normal and primary prostate cancer (Grasso et al., 2012) (Figure S5B). Based upon these genomic data and our finding that NCOR2 represses DUB3 expression in cultured cells (Figure 1), we hypothesized that loss of NCOR due to deletions or mutations results in DUB3 upregulation, which in turn causes BRD4 protein deubiquitination and elevation (Figure 5A). To test this hypothesis, we sought to determine the correlation among expression of NCOR2, DUB3 and BRD4 proteins in human prostate cancer specimens. We examined the expression of these three proteins by

performing immunohistochemistry (IHC) on a tissue microarray (TMA) containing a cohort of prostate cancer samples (n = 53). IHC staining index (SI) was calculated by measuring both percentage of positive staining cells and staining intensity. Representative images of low/no and high staining of NCOR2, DUB3 and BRD4 were shown in Figure 5B. We demonstrated that majority of tumors expressed NCOR2 protein at very low level and NCOR2 expression inversely correlated with the level of DUB3 (Pearson's product-moment correlation co-efficiency $r = -0.334$, $p = 0.0146$) and BRD4 (Pearson's product-moment correlation coefficiency $r = -0.247$, $p = 0.0747$) (Figures 5C–5E). In support of our hypothesis, DUB3 expression positively correlated with BRD4 protein level in this cohort (Pearson's product-moment correlation co-efficiency $r = 0.613$, $p = 1.09e\text{-}6$) (Figure 5F). These data suggest that decreased expression of NCOR2 correlates with increased expression of DUB3 and BRD4 proteins in prostate cancer patient specimens.

We further tested our hypothesis by using cell culture models. We demonstrated that knockdown of NCOR2 by two independent shRNAs increased expression of DUB3 and BRD4, but not BRD2 and BRD3 proteins while NCOR2 knockdown only increased mRNA expression of DUB3, but not BRD4 (Figures 5G and 5H). Moreover, knockdown of endogenous NCOR2 prolonged BRD4 protein half-life and attenuated BRD4 polyubiquitination (Figures 5I–5K). We also examined whether deletion of NCOR2 affects BRD4 protein level through upregulation of DUB3. Knockdown of DUB3 completely abolished NCOR2 depletion-induced elevation of BRD4 protein and BRD4 protein polyubiquitination, but had no effect on BRD4 mRNA expression (Figure 5L–5N and S5C). These data suggest that NCOR2 is a critical upstream regulator of BRD4 protein, effect of which is mediated through DUB3 (Figure 5A).

DUB3-mediated deubiquitination and stability of BRD4 is regulated by CDK4/6

A previous report shows that the catalytic activity of DUB3 relies on CDK4/6-mediated phosphorylation and DUB3-mediated protein deubiquitination is inhibited by CDK4/6 inhibitors (Liu et al., 2017). We therefore examined whether CDK4/6 inhibition affects BRD4 stabilization. By knocking down CDK4 or CDK6 alone or in combination in DU145 cells, we demonstrated that BRD4 protein level was largely reduced by CDK4 or CDK6 knockdown and the effect was more robust in CDK4 and CDK6 co-knockdown cells (Figure 6A). Since DU145 cells contain an abnormally small protein translated from an *RB* messenger RNA that lacks 105 nucleotides encoded by exon 21 (Bookstein et al., 1990), the effect of CDK4/6 depletion on BRD4 expression appears to be RB-independent. PD0332991 is a new-generation selective CDK4/6 inhibitor (Beaver et al., 2015; Finn et al., 2016; O'Leary et al., 2016). Treatment of DU145 cells with PD0332991 decreased BRD4 protein in a time-dependent manner (Figure 6B) and the effect of PD0332991 was completely impeded by the proteasome inhibitor MG132 (Figure 6C), arguing that CDK4/6 inhibitor accelerates BRD4 degradation.

To investigate whether DUB3 regulation of BRD4 relies on CDK4/6 activity, we treated DU145 cells with PD0332991 and demonstrated that PD0332991 treatment completely blocked DUB3-induced upregulation of BRD4 protein (Figure 6D). Moreover, knockdown of DUB3 largely decreased BRD4 protein level, but little or no further reduction in BRD4

protein expression by co-treatment with PD0332991 (Figure 6E). Furthermore, PD0332991 treatment also increased BRD4 polyubiquitination, shortened BRD4 protein half-life, and reversed DUB3-mediated deubiquitination of BRD4 in DU145 cells (Figure 6F–6H).

CDK4/6-mediated serine-41 phosphorylation of DUB3 has been shown to be essential for the catalytic activity of DUB3 (Liu et al., 2017). We demonstrated that knockdown of endogenous DUB3 by two independent shRNAs largely decreased BRD4 protein and these effects were reversed by restored expression of DUB3-WT and the phospho-mimicking mutant S41D, but not the phosphorylation-resistant mutant S41A (Figures 6I and S6A). Similarly, ectopic or restored expression of DUB3-WT and S41D mutant, but not S41A mutant decreased BRD4 polyubiquitination in PC-3 cells (Figures 6J and S6B). Moreover, different from DUB3-WT, overexpression of the S41A mutant failed to prolong the half-life of BRD4 protein in PC-3 cells (Figures 6K and 6L). These data suggest that CDK4/6 phosphorylation of DUB3 is essential for DUB3-mediated deubiquitination and stabilization of BRD4 (Figure 6M).

DUB3 inhibition sensitizes prostate cancer cells to BET inhibitor in vitro and in mice

As described above, JQ1 treatment increased BRD4 expression at the protein, but not mRNA level in prostate cancer cells (Figures 2J–2M). Our data further showed that JQ1 treatment prolonged BRD4 protein half-life (Figure 7A). Given that JQ1 induces upregulation of DUB3 at both mRNA and protein levels in different cell types (Borbely et al., 2015) (Figures 2J–2M) and DUB3 binds to BRD4 and promotes its deubiquitination and protein stabilization (Figures 3 and 4), we sought to determine whether JQ1-induced stabilization of BRD4 is mediated through upregulation of active DUB3. We demonstrated that JQ1-induced upregulation of BRD4 protein was almost completely abolished by DUB3 knockdown or inhibition of DUB3 by CDK4/6 inhibitor PD0332991 (Figures 7B and 7C). Accordingly, JQ1 treatment markedly inhibited BRD4 polyubiquitination, but this effect was almost completely reversed by DUB3 knockdown or PD0332991 (Figures 7D and 7E). These data suggest that BET inhibitor-induced upregulation of DUB3 plays a key role in BET inhibitor-induced stabilization and elevation of BRD4 proteins.

BRD4 stabilization confers resistance to BET inhibitor (Dai et al., 2017; Janouskova et al., 2017; Zhang et al., 2017). We sought to determine whether DUB3 inhibition sensitizes prostate cancer cells to BET inhibitors. Co-treatment of DUB3-proficient, RB-deficient DU145 cells with JQ1 and PD0332991 resulted in much greater inhibitory effect on cell growth in vitro (Figure 7F). Similarly, DUB3-knockdown cells were much more sensitive to JQ1 than the control knockdown cells and most importantly, little or no additive effect of co-treatment of JQ1 and PD0332991 on cell growth was detected in DUB3-knockdown cells (Figures 7F). We obtained similar results when DU145 cells were treated with another BET inhibitor I-BET762 (I-BET) in combination with or without PD0332991 (Figure S6C). Moreover, we performed DUB3 overexpression experiments and demonstrated that overexpression of DUB3 conferred resistance to both JQ1 and I-BET in DU145 cells and these effects were completely abolished by BRD4 knockdown (Figures S6D–S6G). These observations were consistent with the results from colony formation assays that IC50 of JQ1 was substantially increased in DUB3 overexpressing cells compared to control cells (Figures

S6H and S6I). Furthermore, co-treatment with JQ1 and PD0332991 also resulted in much greater inhibition of growth of control DU145 xenograft tumors in mice than each single agent alone, but such effect was recapitulated by JQ1 treatment in combination with DUB3 knockdown (Figures 7G and 7H). These data suggest DUB3 is a critical upstream regulator of BRD4 protein stability and inhibition of DUB3 by CDK4/6 inhibitor overcomes BET inhibitor-induced elevation of BRD4 protein and BET inhibitor resistance in a RB-independent manner (Figure 7I).

We further examined the effect of DUB3 on BRD4 protein degradation and JQ1 sensitivity in SPOP mutated prostate cancer cells. Similar to the previous report (Zhang et al., 2017), expression of SPOP F133V, a hot spot mutant of SPOP largely increased BRD4 levels and caused JQ1 resistance in both DU145 and C4-2 cell lines (Figures S7A–S7D). Unexpectedly, knockdown of DUB3 not only decreased BRD4 protein level in SPOP F133V-expressing DU145 cells, but also sensitized SPOP-F133V cells to JQ1 treatment (Figures S7A-S7D), suggesting the presence of a SPOP-independent putative E3 ligase targeting BRD4 protein for degradation. To test this hypothesis, we examined the effect of DUB3 knockdown on BRD4 protein ubiquitination degradation in SPOP F133V-expressing DU145 and SPOP CRISPR knockout PC-3 cells. We demonstrated that knockdown of DUB3 still enabled to increase BRD4 polyubiquitination in F133V-expressing DU145 cells (Figure S7E). Accordingly, DUB3 knockdown decreased BRD4 protein levels in F133V-expressing cells and this effect was blocked by MG132 (Figures S7F). Similar results were observed in SPOP CRISPR knockout PC-3 cells (Figures S7G and S7H). These data further suggest there exists a SPOP-independent undefined E3 ligase for BRD4 degradation, but also demonstrate that inhibition of DUB3 can overcome SPOP mutation-conferred BET inhibitor resistance (Figures S7A–S7D). Together, our data highlight that targeting DUB3 represents a new strategy to overcome BET inhibitor resistance in SPOP-mutated prostate cancer.

DISSCUSSION

The ubiquitination proteasome system (UPS) plays a critical role in regulating protein stability (Skaar et al., 2014). It has been shown recently that BRD4 is a polyubiquitination target and its polyubiquitination can be mediated by its interaction with the E3 ubiquitin ligase adaptor SPOP (Dai et al., 2017; Janouskova et al., 2017; Zhang et al., 2017). BRD4 protein stability is also regulated by its interaction with prolyl isomerase PIN1 (Hu et al., 2017). However, which DUB(s) promotes BRD4 deubiquitination and stabilization remains unclear. In the present study we demonstrated that DUB3 specifically binds to BRD4 and promotes its deubiquitination. We further showed that forced expression of DUB3 induced upregulation of BRD4 proteins in cultured cells and elevation of DUB3 expression correlated with high level of BRD4 protein in a subset of CRPC patient samples. To our knowledge, DUB3 is the first identified DUB that promotes BRD4 deubiquitination and protein stabilization.

Several small-molecule inhibitors of BRD4 protein are currently in clinical trials for treatment of human cancers (Filippakopoulos et al., 2010; Nicodeme et al., 2010). However, BET inhibitor resistance often emerges in various cancer types (Fong et al., 2015; Rathert et

al., 2015; Shu et al., 2016). Recent studies further show that increased level of BRD4 protein is a key factor that confers resistance to BET inhibitors (Dai et al., 2017; Janouskova et al., 2017; Zhang et al., 2017). In an array of cancer cell lines, we demonstrated that knockdown of DUB3 by shRNAs largely decreased BRD4 protein levels, but not at mRNA level. Importantly, we further showed that DUB3 depletion markedly sensitized prostate cancer cells to BET inhibitors in vitro and in mice. In agreement with the recent report that the deubiquitination activity of DUB3 relies on CDK4/6-mediated phosphorylation of DUB3 and this activity is inhibited by the CDK4/6 inhibitor (Liu et al., 2017), we demonstrated that treatment of mice with the CDK4/6 inhibitor palbociclib largely sensitized DUB3-proficient prostate tumors to JQ1, but the effect of palbociclib was almost completely abolished by DUB3 knockdown. It is worth noting that palbociclib belongs to the new-generation, highly selective CDK4/6 inhibitor and it has been approved for treatment of patients with hormone receptor-positive breast cancer (O'Leary et al., 2016). Palbociclib can also delay proliferation of prostate cancer cells in a RB-dependent manner (Comstock et al., 2013). Thus, our findings stress that increased expression of BRD4 due to DUB3-mediated deubiquitination and stabilization confers resistance to BET inhibitors. However, DUB3 overexpression-mediated JQ1 resistance can be largely diminished by the CDK4/6 inhibitor palbociclib in a manner independent of RB function.

NCOR2 plays critical roles in gene transcription repression by forming a protein complex with class I/II HDAC proteins (Fischer et al., 2002). HDAC10 is a member of the class II HDACs. However, the role of HDAC10 in cancer is largely unclear. We demonstrated that NCOR2 represses DUB3 expression by specifically interacting with HDAC10. It has been shown that the *NCOR2* gene was frequently deleted or mutated in a subset of metastatic prostate cancers and CRPC patients (Cancer Genome Atlas Research, 2015; Robinson et al., 2015). We provided evidence that depletion of NCOR2 by shRNAs increased DUB3 and BRD4 in prostate cancer cells in culture. We further showed that expression of NCOR2 protein was frequently downregulated in a cohort of prostate cancer patients. Most importantly, decreased expression of NCOR2 protein significantly correlated with elevated level of DUB3 and BRD4 in patient samples examined. Our findings predict that patients with tumors containing NCOR2 deletions or mutation may be resistant to BET inhibitors.

It has been well documented that BET inhibitor treatment invariably induces BRD4 protein accumulation in different cell types (Asangani et al., 2014; Lu et al., 2015). It has been shown recently that treatment of the BET inhibitor JQ1 attenuated the interaction of BRD4 with the SPOP E3 ubiquitin ligase and partially impaired SPOP-mediated ubiquitination and degradation of BRD4, thereby providing a partial explanation of how BET inhibitor treatment causes elevation of BRD4 proteins (Zhang et al., 2017). However, the precise underlying mechanism remains elusive. Our findings in the current study show that functioning as a transcriptional repressor NCOR2 represses DUB3 expression. We further show that BRD4 binds to the *NCOR2* gene promoter and induces NCOR2 mRNA expression. In support of these findings, we show that inhibition of BRD4 by JQ1 blocks *NCOR2* mRNA expression, which in turn dismisses NCOR2-mediated repression of DUB3 and DUB3-mediated deubiquitination of BRD4. Thus, our findings identify a new mechanism explaining how inhibition of BRD4 activity results in elevation of BRD4 at protein, but not mRNA level.

In summary, we identify DUB3 as the first deubiquitinase that promotes BRD4 deubiquitination and stabilization. We also show that expression of DUB3 is negatively regulated by the NCOR2-HDAC10 complex. Importantly, the *NCOR2* gene is often deleted or mutated in a subset of metastatic CRPC patient specimens and expression of NCOR2 protein inversely correlates with DUB3 and BRD4 protein levels. Furthermore, we demonstrate both in vitro and in mice that DUB3-proficient prostate cancer cells are resistant to JQ1 and the resistance is abolished by the DUB3 inhibitory agents such as CDK4/6 inhibitor in a manner independent of RB. Thus, our findings reveal a previously uncharacterized NCOR2/HDAC10-DUB3 signaling pathway that governs BRD4 protein levels and bromodomain inhibitor sensitivity (Figure 7I). Our data suggest that deregulation of this signaling axis, such as frequent deletions or mutations in the *NCOR2* genes in human cancers including prostate cancer can cause resistance to BET inhibitors. Importantly, we also provide evidence that targeting DUB3 can offer a viable therapeutic option to overcome BET inhibitor resistance in tumors with deregulated NCOR2/HDAC10-DUB3-BRD4 signaling axis or SPOP mutations.

STAR★METHODS

KEY RESOURCES TABLE

REAGENT or RESOURCE	SOURCE	IDENTIFIER
Antibodies		
Mouse monoclonal anti-USP7	Santa Cruz	Cat# sc-137008
Rabbit polyclonal anti-DUB3	Abcam	Cat# ab129931
Mouse monoclonal anti-USP10	Santa Cruz	Cat# sc-365828
Mouse monoclonal anti-USP13	Santa Cruz	Cat# sc-514416
Mouse monoclonal anti-USP15	Santa Cruz	Cat# sc-100629
Rabbit polyclonal anti-USP28	Cell Signaling Technology	Cat# 4217S
Rabbit polyclonal anti-USP49	Abcam	Cat# ab127547
Rabbit monoclonal anti-BRD4	Abcam	Cat# ab128874
Rabbit monoclonal anti-BRD2	Abcam	Cat# ab139690
Rabbit polyclonal anti-BRD3	Bethyl Laboratories	Cat# A302-368A
Rabbit polyclonal anti-HDAC10	Abcam	Cat# ab53096
Rabbit polyclonal anti-NCOR2	Abcam	Cat# ab24551
Rabbit polyclonal anti-SPOP	Proteintech	Cat# 16750-1-AP
Mouse monoclonal anti-ERK2	Santa Cruz	Cat# sc-135900
Mouse monoclonal anti-c-Myc	Santa Cruz	Cat# sc-40
Mouse monoclonal anti-FLAG M2	Sigma-Aldrich	Cat#F-3165
Mouse monoclonal anti-HA.11	Covance	Cat#MMS-101R
Peroxidase IgG Fraction Monoclonal Mouse Anti-Rabbit IgG	Jackson ImmunoResearch	Cat#211-032-171
Peroxidase AffiniPure Goat Anti-Mouse IgG	Jackson ImmunoResearch	Cat#115-035-174
Bacterial and Virus Strains		

REAGENT or RESOURCE	SOURCE	IDENTIFIER
E. coli DH5α	Thermo Fisher	Cat#18258012
E. coli BL21	Thermo Fisher	Cat#C600003
lentivirus-expressing HDAC10-shRNAs	Sigma-Aldrich	SHCLNG-NM_032019
lentivirus-expressing NCOR2-shRNAs	Sigma-Aldrich	SHCLNG-NM 006312
lentivirus-expressing BRD4-shRNAs	Sigma-Aldrich	SHCLNG-NM_058243
lentivirus-expressing SPOP-shRNAs	Sigma-Aldrich	SHCLNG-NM_025287
Chemicals, Peptides, and Recombinant Proteins		
MG132	Sigma-Aldrich	Cat#M8699
Cycloheximide	Sigma-Aldrich	Cat#01810
JQ1	Sigma-Aldrich	Cat#SML1524
Lipofectamine 2000 reagent	Thermo Fisher	Cat#11668500
I-BET762	Selleckchem	Cat# S7189
PD0332991	Selleckchem	Cat# S1116
Critical Commercial Assays		
KOD Plus Mutagenesis Kit	Toyobo	Cat# F0936K
Deposited Data		
Raw data and images	This paper and Mendeley Data	http://dx.doi.org/10.17632/s83f5y9ntt.1
Experimental Models: Cell Lines		
Human: C4-2	Uro Corporation	N/A
Human: PC-3	ATCC	CRL-1435
Human: DU145	ATCC	HTB-81
Human: HEK293T	ATCC	CRL-11268
Human: MIA PaCa-2	ATCC	CRL-1420
Human: MCF7	ATCC	HTB-22
Human: MDA-MB-231	ATCC	HTB-26
Human: MDA-MB-436	ATCC	HTB-130
Human: PANC-1	ATCC	CRL-1469
Human: 22Rv1	ATCC	CRL-2505
Oligonucleotides		
See Table S1 for primer sequences		
Recombinant DNA		
Flag-DUB3	Dr. Zhenkun Lou	(Liu et al., 2017)
HA-DUB3	Dr. Zhenkun Lou	(Liu et al., 2017)
Flag-BRD3	Dr. S. Jane Flint	(LeRoy et al., 2008)
Flag-BRD2	Dr. S. Jane Flint	(LeRoy et al., 2008)
Flag-BRD4	Dr. Tasuku Honjo	(Stanlie et al., 2014)
Flag-USP7	Dr. Zhenkun Lou	(Yuan et al., 2010)
Flag-USP10	Dr. Zhenkun Lou	(Yuan et al., 2010)
Flag-USP13	Dr. Zhenkun Lou	(Yuan et al., 2010)

REAGENT or RESOURCE	SOURCE	IDENTIFIER
Flag-USP15	Dr. Zhenkun Lou	(Yuan et al., 2010)
Flag-USP28	Dr. Zhenkun Lou	(Yuan et al., 2010)
Flag-USP49	Addgene	Cat##22586
Software and Algorithms		
ImageJ	NIH	N/A
GraphPad Prism 5.0	Graphpad, Inc	N/A

CONTACT FOR REAGENT AND RESOURCE SHARING

Further information and requests for resources and reagents should be directed to and will be fulfilled by the Lead Contact Haojie Huang (huang.haojie@mayo.edu).

EXPERIMENTAL MODEL AND SUBJECT DETAILS

Cell culture and transfection—C4-2, PC-3 and DU145 cells were cultured in RPMI medium supplemented with 10% fetal bovine serum (FBS). 293T cells were cultured in DMEM medium supplementary with 10% FBS. All cell lines were kept in a 37°C incubator at 5% CO_2. Transfections were performed by using Lipofectamine 2000 (Thermo Fisher Scientific).

RNA interference—Lentivirus-based control and gene-specific small hairpin RNAs (shRNAs) were purchased from Sigma-Aldrich. Viral packaging plasmids (pEXQV and pVSV-G) and shRNA plasmid were transfected to 293T cells by using Lipofectamine 2000. After 24 h, virus culture medium was replaced with DMEM containing 10% FBS with 1:100 of sodium Pyruvate. 48 h post transfection, medium was collected and added to prostate cancer cells added with 12 μg/ml of polybrene. Prostate cancer cells were harvested 48 h after puromycin selection. shRNA sequence information is provided in Supplementary Table S1.

Tissue microarray and immunohistochemistry (IHC) scoring—The prostate cancer tissue microarray (TMA) slides including 53 cases of prostate cancer TMA specimens, were stained with NCOR2, BRD4 and DUB3 antibodies by standard immunohistochemistry procedures. The IHC staining was scored based on staining intensity and ratio of positive cells as described previously (Jin et al., 2017). A final IHC staining index (SI) score for each specimen was determined using the following formula: ratio of positive cells intensity.

Co-immunoprecipitation (co-IP)—Cells were harvested and lysed by IP buffer (50 mM Tris-HCl, pH 7.4, 150 mM NaCl, 1% Triton X-100, 1% sodium deoxycholate and 1% protease inhibitor cocktails) on ice for more than 15 min. Cell lysate was centrifuged for 15 min at 13,000 rpm at 4°C, and the supernatant was incubated with primary antibodies and protein A/G agarose beads (Thermo Fisher Scientific) with rotating at 4°C overnight. The next day, the pellet was washed at least six times with 1×IP buffer on ice, and then subjected to western blotting analysis.

Western blotting—Cells were harvested and lysed by IP buffer (50 mM Tris-HCl, pH 7.4, 150 mM NaCl, 1% Triton X-100, 1% sodium deoxycholate and 1% protease inhibitor cocktails) on ice for more than 15 min. Cell lysate was centrifuged for 15 min at 13,000 rpm at 4°C, and the supernatant was quantified by BCA protein quantification assay. Equal amounts of protein sample were added into 4× sample buffer and boiled for 5min. The sample was subjected to SDS-PAGE analysis and transferred to nitrocellulose membrane. The membrane was blocked by 5% milk for 1 h at room temperature and incubated with primary antibody at 4°C overnight. The next day, the membrane was washed three times with 1×TBST and incubated with horseradish peroxidase-conjugated secondary antibodies for 1 h at room temperature. The protein bands were visualized by SuperSignal West Pico Stable Peroxide Solution (Thermo Fisher Scientific).

Quantitative RT-PCR—Total RNA was isolated using TRIzol reagent (Thermo Fisher Scientific). The NanoDrop 2000 spectrophotometer (Thermo Fisher Scientific) was used to assess RNA yield and quality. RNA was reversely transcribed using Superscript II reverse transcriptase (Thermo Fisher Scientific) following manufacturer's instructions. Quantitative real-time PCR was performed by mixing cDNA, gene-specific primers and IQ SYRB Green Supermix and detected by iCycler QTX detection system (Bio-Rad). The 2-ΔCt method was used to quantitate fold changes by normalizing to *GAPDH*. Primer for RT-qPCR is provided in Supplementary Table S1.

Chromatin immunoprecipitation (ChIP) and ChIP-reChIP assay—ChIP was performed as described previously (Boyer et al., 2005). For ChIP-reChIP assay DNA, cell lysates were sonicated and subjected to immunoprecipitation using NCOR2 antibody. After washed by RIPA buffer (50 mM Hepes-KOH, pH 7.6, 500 mM LiCl, 1 mM EDTA, 1% NP-40, 0.7% Na-Deoxycholate), the protein-DNA complexes were eluted by elution buffer (10 mM Tris, 1 mM EDTA, 2% SDS, and 20 mM DTT, PH 7.5) for 30 min at 37°C. Then, the supernatant was diluted 20 times and subjected to the second ChIP using IgG or HDAC10 antibodies using the method described previously (Li et al., 2014). DNA pulled down by antibodies or nonspecific IgG was amplified by real-time PCR. The information for ChIP primers is provided in Supplementary Table S1.

Cell proliferation—Cell proliferation was measured by using the MTS assay (Promega). Prostate cancer cells (2,000 per well) were seeded in 96-well plates with 100 μl of culture medium. Each well was added with 20 μl of CellTiter 96R AQueous One Solution Reagent (Promega) and absorbance was measured in a microplate reader at 490 nm.

Colony formation assay—An appropriate number of cells for different dosages of JQ1 were plated onto 6-well plate and treated with JQ1 for three days. After three-day treatment, the medium was changed with fresh medium without drugs for another 8 days. The colonies were fixed with acetic acid: methanol (1:7) for 30 mins and stained with crystal violet (0.5% w/v) for 1 h. Colonies with more than 50 cells were counted. The linear regression was applied to generate the survival curve.

Generation and treatment of prostate cancer xenografts in mice—6-week-old NOD-SCID IL-2-receptor gamma null (NSG) mice were generated in house and used for

animal experiments. The animal study was approved by the IACUC at Mayo Clinic. All mice were housed in standard conditions with a 12 h light/dark cycle and access to food and water ad libitum. For studies with tumors treated with JQ1 and the CDK4/6 inhibitor PD0332991, DU145 cells (5×10^6) infected with lentivirus expression shRNA control or DUB3-specific shRNA (in 50 μl 1×PBS plus 50 μl Matrigel (BD Biosciences)) were injected s.c. into the right flank of mice. After xenografts reached a size of approximately 100 mm^3, vehicle (10% β-cyclodextrin (intraperitoneal injection) and saline (oral administration)), JQ1 (50 mg per kg bodyweight (intraperitoneal injection)) and PD0332991 (150 mg per kg bodyweight (oral administration)) were administrated individually or in combination 5 days per week. The volume of xenografts was measured every other day for 21 days and estimated using the formula $L\times W^2\times0.5$ (L: length, W: width). Upon the completion of measurement, tumor grafts were harvested.

QUANTIFICATION AND STATISTICAL ANALYSIS

All values were expressed as means±SD. Statistical analyses were performed with Student t test for single comparison and one way ANOVA and a post hoc test for multiple comparisons. *P* values < 0.05 are considered statistically significant. Pearson's product-moment correlation was used to calculate the correlation between NCOR2, BRD4 and DUB3 staining index in prostate cancer TMAs.

DATA AND SOFTWARE AVAILABILITY

Original images of western blot data are available at Mendeley Data under the following link: http://dx.doi.org/10.17632/s83f5y9ntt.1.

Supplementary Material

Refer to Web version on PubMed Central for supplementary material.

Acknowledgments

We thank the patients and their families for their altruism in participating in research studies. This work was supported in part by grants from the National Institutes of Health (CA134514, CA130908, CA193239, and CA203849 to H.H.) and the National Natural Science Foundation of China (81702374 to X.J.).

References

Asangani IA, Dommeti VL, Wang X, Malik R, Cieslik M, Yang R, Escara-Wilke J, Wilder-Romans K, Dhanireddy S, Engelke C, et al. Therapeutic targeting of BET bromodomain proteins in castration-resistant prostate cancer. Nature. 2014; 510:278–282. [PubMed: 24759320]

Beaver JA, Amiri-Kordestani L, Charlab R, Chen W, Palmby T, Tilley A, Zirkelbach JF, Yu J, Liu Q, Zhao L, et al. FDA Approval: Palbociclib for the Treatment of Postmenopausal Patients with Estrogen Receptor-Positive, HER2-Negative Metastatic Breast Cancer. Clin Cancer Res. 2015; 21:4760–4766. [PubMed: 26324739]

Blee AM, Liu S, Wang L, Huang H. BET bromodomain-mediated interaction between ERG and BRD4 promotes prostate cancer cell invasion. Oncotarget. 2016; 7:38319–38332. [PubMed: 27223260]

Bookstein R, Shew JY, Chen PL, Scully P, Lee WH. Suppression of tumorigenicity of human prostate carcinoma cells by replacing a mutated RB gene. Science. 1990; 247:712–715. [PubMed: 2300823]

Borbely G, Haldosen LA, Dahlman-Wright K, Zhao C. Induction of USP17 by combining BET and HDAC inhibitors in breast cancer cells. Oncotarget. 2015; 6:33623–33635. [PubMed: 26378038]

Boyer LA, Lee TI, Cole MF, Johnstone SE, Levine SS, Zucker JP, Guenther MG, Kumar RM, Murray HL, Jenner RG, et al. Core transcriptional regulatory circuitry in human embryonic stem cells. Cell. 2005; 122:947–956. [PubMed: 16153702]

Cancer Genome Atlas Research N. The Molecular Taxonomy of Primary Prostate Cancer. Cell. 2015; 163:1011–1025. [PubMed: 26544944]

Comstock CE, Augello MA, Goodwin JF, de Leeuw R, Schiewer MJ, Ostrander WF Jr, Burkhart RA, McClendon AK, McCue PA, Trabulsi EJ, et al. Targeting cell cycle and hormone receptor pathways in cancer. Oncogene. 2013; 32:5481–5491. [PubMed: 23708653]

Dai X, Gan W, Li X, Wang S, Zhang W, Huang L, Liu S, Zhong Q, Guo J, Zhang J, et al. Prostate cancer-associated SPOP mutations confer resistance to BET inhibitors through stabilization of BRD4. Nat Med. 2017; 23:1063–1071. [PubMed: 28805820]

Dali-Youcef N, Froelich S, Moussallieh FM, Chibbaro S, Noel G, Namer IJ, Heikkinen S, Auwerx J. Gene expression mapping of histone deacetylases and co-factors, and correlation with survival time and 1H-HRMAS metabolomic profile in human gliomas. Sci Rep. 2015; 5:9087. [PubMed: 25791281]

Delmore JE, Issa GC, Lemieux ME, Rahl PB, Shi J, Jacobs HM, Kastritis E, Gilpatrick T, Paranal RM, Qi J, et al. BET bromodomain inhibition as a therapeutic strategy to target c-Myc. Cell. 2011; 146:904–917. [PubMed: 21889194]

Deng M, Yang X, Qin B, Liu T, Zhang H, Guo W, Lee SB, Kim JJ, Yuan J, Pei H, et al. Deubiquitination and Activation of AMPK by USP10. Mol Cell. 2016; 61:614–624. [PubMed: 26876938]

Filippakopoulos P, Qi J, Picaud S, Shen Y, Smith WB, Fedorov O, Morse EM, Keates T, Hickman TT, Felletar I, et al. Selective inhibition of BET bromodomains. Nature. 2010; 468:1067–1073. [PubMed: 20871596]

Finn RS, Martin M, Rugo HS, Jones S, Im SA, Gelmon K, Harbeck N, Lipatov ON, Walshe JM, Moulder S, et al. Palbociclib and Letrozole in Advanced Breast Cancer. N Engl J Med. 2016; 375:1925–1936. [PubMed: 27959613]

Fischer DD, Cai R, Bhatia U, Asselbergs FA, Song C, Terry R, Trogani N, Widmer R, Atadja P, Cohen D. Isolation and characterization of a novel class II histone deacetylase, HDAC10. J Biol Chem. 2002; 277:6656–6666. [PubMed: 11739383]

Floyd SR, Pacold ME, Huang Q, Clarke SM, Lam FC, Cannell IG, Bryson BD, Rameseder J, Lee MJ, Blake EJ, et al. The bromodomain protein Brd4 insulates chromatin from DNA damage signalling. Nature. 2013; 498:246–250. [PubMed: 23728299]

Fong CY, Gilan O, Lam EY, Rubin AF, Ftouni S, Tyler D, Stanley K, Sinha D, Yeh P, Morison J, et al. BET inhibitor resistance emerges from leukaemia stem cells. Nature. 2015; 525:538–542. [PubMed: 26367796]

Grasso CS, Wu YM, Robinson DR, Cao X, Dhanasekaran SM, Khan AP, Quist MJ, Jing X, Lonigro RJ, Brenner JC, et al. The mutational landscape of lethal castration-resistant prostate cancer. Nature. 2012; 487:239–243. [PubMed: 22722839]

Hu X, Dong SH, Chen J, Zhou XZ, Chen R, Nair S, Lu KP, Chen LF. Prolyl isomerase PIN1 regulates the stability, transcriptional activity and oncogenic potential of BRD4. Oncogene. 2017; 36:5177–5188. [PubMed: 28481868]

Jang MK, Mochizuki K, Zhou M, Jeong HS, Brady JN, Ozato K. The bromodomain protein Brd4 is a positive regulatory component of P-TEFb and stimulates RNA polymerase II-dependent transcription. Mol Cell. 2005; 19:523–534. [PubMed: 16109376]

Janouskova H, El Tekle G, Bellini E, Udeshi ND, Rinaldi A, Ulbricht A, Bernasocchi T, Civenni G, Losa M, Svinkina T, et al. Opposing effects of cancer-type-specific SPOP mutants on BET protein degradation and sensitivity to BET inhibitors. Nat Med. 2017; 23:1046–1054. [PubMed: 28805821]

Jin X, Pan Y, Wang L, Ma T, Zhang L, Tang AH, Billadeau DD, Wu H, Huang H. Fructose-1,6-bisphosphatase Inhibits ERK Activation and Bypasses Gemcitabine Resistance in Pancreatic Cancer by Blocking IQGAP1-MAPK Interaction. Cancer Res. 2017; 77:4328–4341. [PubMed: 28720574]

Korb E, Herre M, Zucker-Scharff I, Darnell RB, Allis CD. BET protein Brd4 activates transcription in neurons and BET inhibitor Jq1 blocks memory in mice. Nat Neurosci. 2015; 18:1464–1473. [PubMed: 26301327]

LeRoy G, Rickards B, Flint SJ. The double bromodomain proteins Brd2 and Brd3 couple histone acetylation to transcription. Mol Cell. 2008; 30:51–60. [PubMed: 18406326]

Li B, Qiu B, Lee DS, Walton ZE, Ochocki JD, Mathew LK, Mancuso A, Gade TP, Keith B, Nissim I, et al. Fructose-1,6-bisphosphatase opposes renal carcinoma progression. Nature. 2014; 513:251–255. [PubMed: 25043030]

Liu T, Yu J, Deng M, Yin Y, Zhang H, Luo K, Qin B, Li Y, Wu C, Ren T, et al. CDK4/6-dependent activation of DUB3 regulates cancer metastasis through SNAIL1. Nat Commun. 2017; 8:13923. [PubMed: 28067227]

Lu J, Qian Y, Altieri M, Dong H, Wang J, Raina K, Hines J, Winkler JD, Crew AP, Coleman K, et al. Hijacking the E3 Ubiquitin Ligase Cereblon to Efficiently Target BRD4. Chem Biol. 2015; 22:755–763. [PubMed: 26051217]

Nicodeme E, Jeffrey KL, Schaefer U, Beinke S, Dewell S, Chung CW, Chandwani R, Marazzi I, Wilson P, Coste H, et al. Suppression of inflammation by a synthetic histone mimic. Nature. 2010; 468:1119–1123. [PubMed: 21068722]

O'Leary B, Finn RS, Turner NC. Treating cancer with selective CDK4/6 inhibitors. Nat Rev Clin Oncol. 2016; 13:417–430. [PubMed: 27030077]

Pereg Y, Liu BY, O'Rourke KM, Sagolla M, Dey A, Komuves L, French DM, Dixit VM. Ubiquitin hydrolase Dub3 promotes oncogenic transformation by stabilizing Cdc25A. Nat Cell Biol. 2010; 12:400–406. [PubMed: 20228808]

Rathert P, Roth M, Neumann T, Muerdter F, Roe JS, Muhar M, Deswal S, Cerny-Reiterer S, Peter B, Jude J, et al. Transcriptional plasticity promotes primary and acquired resistance to BET inhibition. Nature. 2015; 525:543–547. [PubMed: 26367798]

Robinson D, Van Allen EM, Wu YM, Schultz N, Lonigro RJ, Mosquera JM, Montgomery B, Taplin ME, Pritchard CC, Attard G, et al. Integrative Clinical Genomics of Advanced Prostate Cancer. Cell. 2015; 162:454. [PubMed: 28843286]

Roe JS, Mercan F, Rivera K, Pappin DJ, Vakoc CR. BET Bromodomain Inhibition Suppresses the Function of Hematopoietic Transcription Factors in Acute Myeloid Leukemia. Mol Cell. 2015; 58:1028–1039. [PubMed: 25982114]

Sakamaki JI, Wilkinson S, Hahn M, Tasdemir N, O'Prey J, Clark W, Hedley A, Nixon C, Long JS, New M, et al. Bromodomain Protein BRD4 Is a Transcriptional Repressor of Autophagy and Lysosomal Function. Mol Cell. 2017; 66:517–532 e519. [PubMed: 28525743]

Shi J, Vakoc CR. The mechanisms behind the therapeutic activity of BET bromodomain inhibition. Mol Cell. 2014; 54:728–736. [PubMed: 24905006]

Shi J, Wang Y, Zeng L, Wu Y, Deng J, Zhang Q, Lin Y, Li J, Kang T, Tao M, et al. Disrupting the interaction of BRD4 with diacetylated Twist suppresses tumorigenesis in basal-like breast cancer. Cancer Cell. 2014; 25:210–225. [PubMed: 24525235]

Shu S, Lin CY, He HH, Witwicki RM, Tabassum DP, Roberts JM, Janiszewska M, Huh SJ, Liang Y, Ryan J, et al. Response and resistance to BET bromodomain inhibitors in triple-negative breast cancer. Nature. 2016; 529:413–417. [PubMed: 26735014]

Skaar JR, Pagan JK, Pagano M. SCF ubiquitin ligase-targeted therapies. Nat Rev Drug Discov. 2014; 13:889–903. [PubMed: 25394868]

Stanlie A, Yousif AS, Akiyama H, Honjo T, Begum NA. Chromatin reader Brd4 functions in Ig class switching as a repair complex adaptor of nonhomologous end-joining. Mol Cell. 2014; 55:97–110. [PubMed: 24954901]

Turnbull AP, Ioannidis S, Krajewski WW, Pinto-Fernandez A, Heride C, Martin ACL, Tonkin LM, Townsend EC, Buker SM, Lancia DR, et al. Molecular basis of USP7 inhibition by selective small-molecule inhibitors. Nature. 2017; 550:481–486. [PubMed: 29045389]

Urbanucci A, Barfeld SJ, Kytola V, Itkonen HM, Coleman IM, Vodak D, Sjoblom L, Sheng X, Tolonen T, Minner S, et al. Androgen Receptor Deregulation Drives Bromodomain-Mediated Chromatin Alterations in Prostate Cancer. Cell Rep. 2017; 19:2045–2059. [PubMed: 28591577]

Wang CY, Filippakopoulos P. Beating the odds: BETs in disease. Trends Biochem Sci. 2015; 40:468–479. [PubMed: 26145250]

Wang D, Garcia-Bassets I, Benner C, Li W, Su X, Zhou Y, Qiu J, Liu W, Kaikkonen MU, Ohgi KA, et al. Reprogramming transcription by distinct classes of enhancers functionally defined by eRNA. Nature. 2011; 474:390–394. [PubMed: 21572438]

Wu Y, Wang Y, Lin Y, Liu Y, Wang Y, Jia J, Singh P, Chi YI, Wang C, Dong C, et al. Dub3 inhibition suppresses breast cancer invasion and metastasis by promoting Snail1 degradation. Nat Commun. 2017; 8:14228. [PubMed: 28198361]

Wu Y, Wang Y, Yang XH, Kang T, Zhao Y, Wang C, Evers BM, Zhou BP. The deubiquitinase USP28 stabilizes LSD1 and confers stem-cell-like traits to breast cancer cells. Cell Rep. 2013; 5:224–236. [PubMed: 24075993]

Yuan J, Luo K, Zhang L, Cheville JC, Lou Z. USP10 regulates p53 localization and stability by deubiquitinating p53. Cell. 2010; 140:384–396. [PubMed: 20096447]

Zhang P, Wang D, Zhao Y, Ren S, Gao K, Ye Z, Wang S, Pan CW, Zhu Y, Yan Y, et al. Intrinsic BET inhibitor resistance in SPOP-mutated prostate cancer is mediated by BET protein stabilization and AKT-mTORC1 activation. Nat Med. 2017; 23:1055–1062. [PubMed: 28805822]

Zhang Z, Jones A, Joo HY, Zhou D, Cao Y, Chen S, Erdjument-Bromage H, Renfrow M, He H, Tempst P, et al. USP49 deubiquitinates histone H2B and regulates cotranscriptional pre-mRNA splicing. Genes Dev. 2013; 27:1581–1595. [PubMed: 23824326]

Highlights

- DUB3 functions as a bona fide deubiquitinase promoting BRD4 deubiquitination
- DUB3 expression is transcriptionally repressed by the NCOR2-HDAC10 complex
- NCOR2 loss correlates with elevated DUB3 and BRD4 protein in cancer specimens
- DUB3 overexpression confers BET inhibitor resistance in cancer cells in vivo

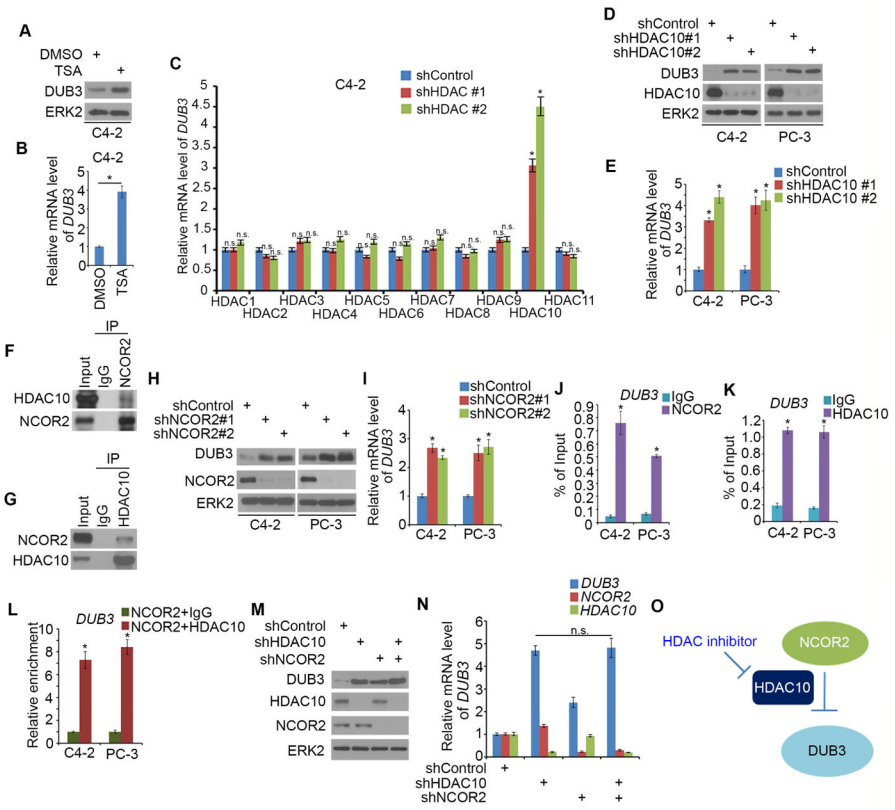

Figure 1. NCOR2 and HDAC10 transcriptionally repress DUB3 expression

(A,B), C4-2 cells were treated with or without TSA (1 μM) for 24 h for Western blot (A) and RT-qPCR (B). ERK2, a loading control. * $P < 0.05$.

(C), C4-2 cells were infected with lentivirus expressing indicated shRNAs for 48 h for RT-qPCR. Data are shown as mean ± SD (n=3). * $P < 0.05$, n.s., not significant comparing to shControl.

(D, E), C4-2 and PC-3 cells were infected with lentivirus expressing indicated shRNAs for 48 h for Western blot (D) and RT-qPCR (E). Data are shown as mean ± SD (n=3). * $P < 0.05$.

(F, G), Western blot analysis of reciprocal co-immunoprecipitation of endogenous proteins in C4-2 cells.

(H, I), C4-2 and PC-3 cells were infected with lentivirus expressing indicated shRNAs for 48h for Western blot (H) and RT-qPCR (I). Data are shown as mean ± SD (n=3). * $P < 0.05$.

(J, K), ChIP-qPCR analysis of NCOR2 (J) and HDAC10 (K) binding at the *DUB3* gene promotor in C4-2 and PC-3 cells. Data are shown as mean ± SD (n=3). * $P < 0.05$.

(L), ChIP-reChIP analysis examining the co-localization of HDAC10 and NCOR2 in the *DUB3* gene promoters in C4-2 and PC-3 cells. Data are shown as mean ± SD (n=3). * $P < 0.05$.

(M, N), C4-2 cells were infected with lentivirus expressing indicated shRNAs for 48 h for Western blot (M) and RT-qPCR (N). Data are shown as mean ± SD (n=3). n.s., not significant.

(O), a hypothetical model depicting transcription repression of DUB3 by NCOR2 and HDAC10.

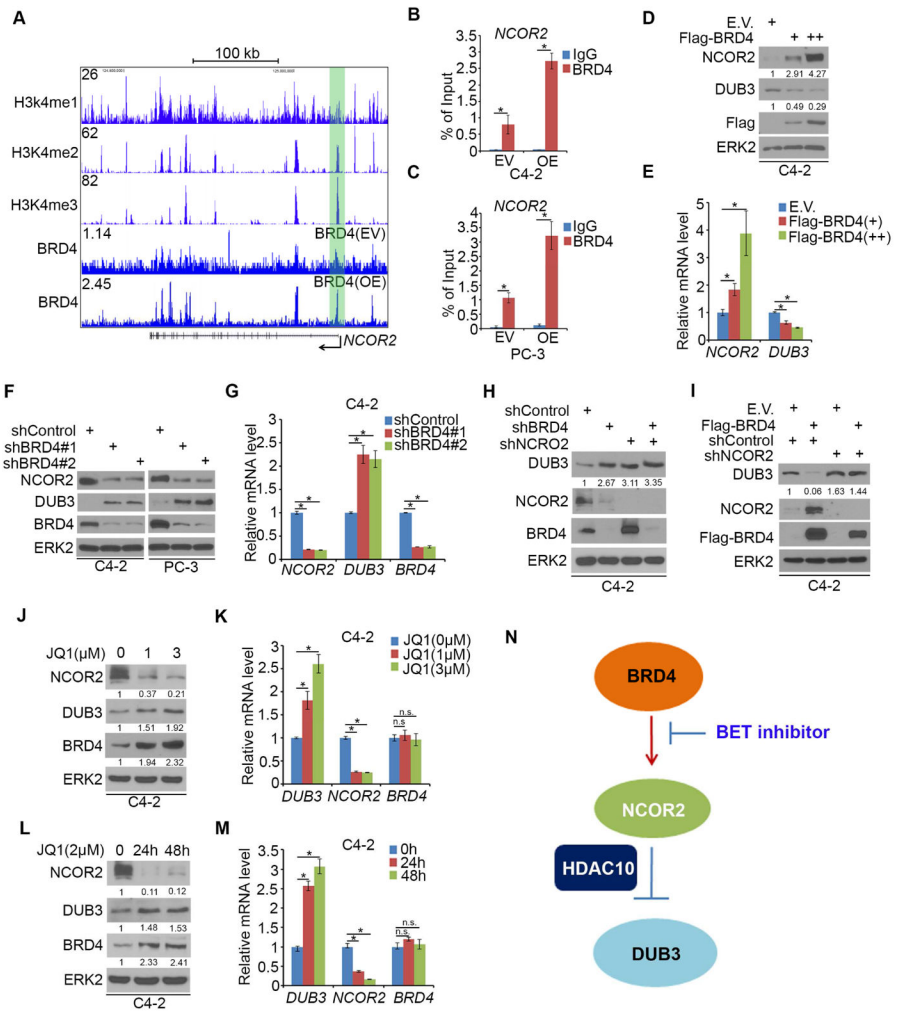

Figure 2. BRD4 represses DUB3 expression via transcriptionally activating NCOR2

(A), UCSC Genome Browser screenshots for BRD4 ChIP–seq profiles in the *DUB3* gene locus in C4-2 cells reported previously (Zhang et al., 2017). H3K4me1, H3K4me2, H3K4me3 ChIP-seq data were reported previously (Wang et al., 2011).

(B, C), ChIP-qPCR analysis of BRD4 binding at the *DUB3* gene promotor in C4-2 (B) and PC-3 cells (C). Data are shown as mean ± SD (n=3). * $P < 0.001$.

(D, E), C4-2 cells were transfected with indicated plasmids for 24 h for Western blot (D) and RT-qPCR (E). Data are shown as mean ± SD (n=3). * $P < 0.05$.

(F), Western blot analysis in C4-2 and PC-3 cells 48 h after infected with indicated shRNAs.

(G), RT-qPCR analysis in C4-2 cells 48 h post infected with indicated shRNAs. Data are shown as mean ± SD (n=3). * $P < 0.05$.

(H), Western blot analysis in C4-2 cells 48 h post infected with indicated shRNAs. DUB3 proteins were quantified by ImageJ software.

(I), C4-2 cells were infected with indicated shRNAs for 24 h and further transfected with plasmids for another 24 h for Western blot.

(J, K), C4-2 cells were treated JQ1 for 24 h for Western blot (J) and RT-qPCR (K). Data are shown as mean ± SD (n=3). * $P < 0.05$. n.s., not significant.

(L, M), C4-2 cells were treated with or without JQ1 for indicated periods for Western blot (J) and RT-qPCR (K). Data are shown as mean ± SD (n=3). * $P < 0.05$.
(N), a hypothetical model depicting that BRD4 represses DUB3 expression via transcriptionally activating NCOR2.

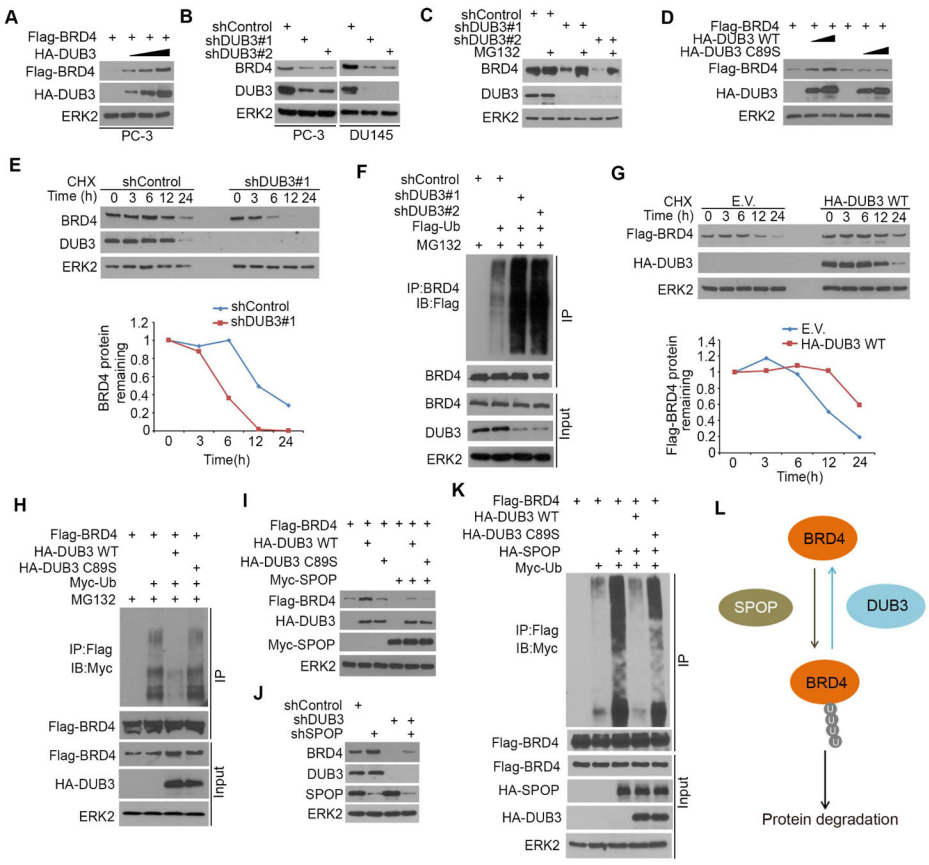

Figure 3. DUB3 deubiquitinates and antagonizes SPOP-mediated ubiquitination of BRD4

(A), Western blot analysis in PC-3 cells 24 h after transfected with indicated plasmids.

(B), Western blot analysis in PC-3 and DU145 cells 48 h after infected with indicated shRNAs.

(C), PC-3 cells were infected with indicated shRNAs for 48 h for Western blot. Cells were treated with MG132 for 8 h before harvested.

(D), Western blot analysis in PC-3 cells 24 h after transfected with indicated plasmids.

(E), PC-3 cells were infected with indicated shRNA for 48 h followed by treatment with 50 μg/μl cycloheximide (CHX) for Western blot. At each time point, the intensity of BRD4 was normalized to the intensity of ERK2 (loading control) first and then to the value at the 0-h time point.

(F), Western blot analysis in PC-3 cells transfected with indicated shRNAs for 48 h for Western blot. Cells were treated with MG132 for 8 h before harvested.

(G), PC-3 cells were transfected with indicated plasmids for 24 h followed by treatment of 50 μg/μl CHX for Western blot. Protein bands were quantified as in (E).

(H), Western blot analysis in PC-3 cells transfected with the indicated plasmids for 24 h. Cells were treated with MG132 for 8 h before harvested.

(I), Western blot analysis in PC-3 cells 24 h after transfected with the indicated plasmids.

(J), Western blot analysis in PC-3 cells 48 h post infected with indicated shRNAs.

(K), Western blot analysis in PC-3 cells transfected with the indicated plasmids for 24 h. Cells were treated with MG132 for 8 h before harvested.

(L), a hypothetical model depicting that DUB3 deubiquitinates and antagonizes SPOP-mediated ubiquitination of BRD4.

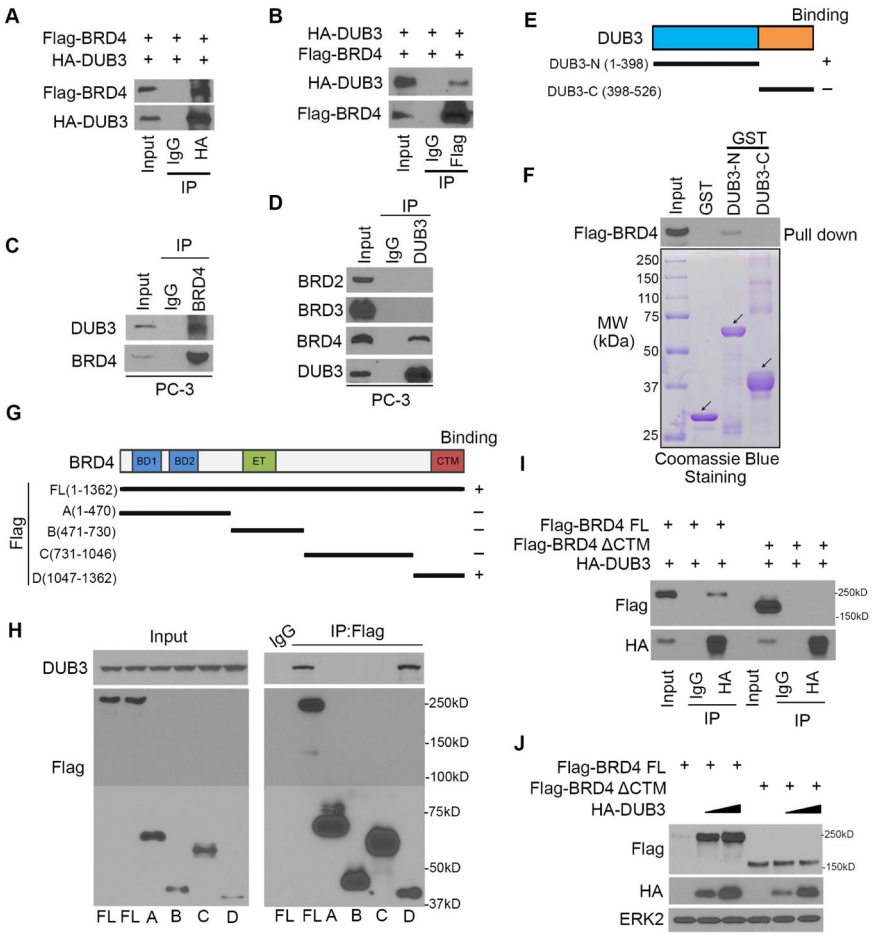

Figure 4. DUB3 interacts with BRD4 in prostate cancer cells

(A, B), Western blot analysis of co-immunoprecipitated proteins from 293T cells transfected with Flag-BRD4 and HA-DUB3.

(C, D), Western blot analysis of co-immunoprecipitated endogenous BRD2/3/4 and DUB3 proteins in PC-3 cells.

(E), schematic diagram depicting a set of GST-DUB3 recombinant protein constructs.

(F), Western blot analysis of Flag-BRD4 proteins in PC-3 cells pulled down by GST or GST-DUB3 recombinant proteins. Arrows indicate the protein bands at the expected molecular weight.

(G), schematic diagram depicting a set of Flag-tagged BRD4 expression constructs.

(H), Western blot analysis of DUB3 proteins in PC-3 cells immunoprecipitated by Flag-BRD4.

(I), Western blot analysis of proteins immunoprecipitated by ectopically expressed Flag-BRD4 or Flag-BRD4 CTM in 293T cells.

(J), Western blot analysis in PC-3 cells transfected with indicated plasmids.

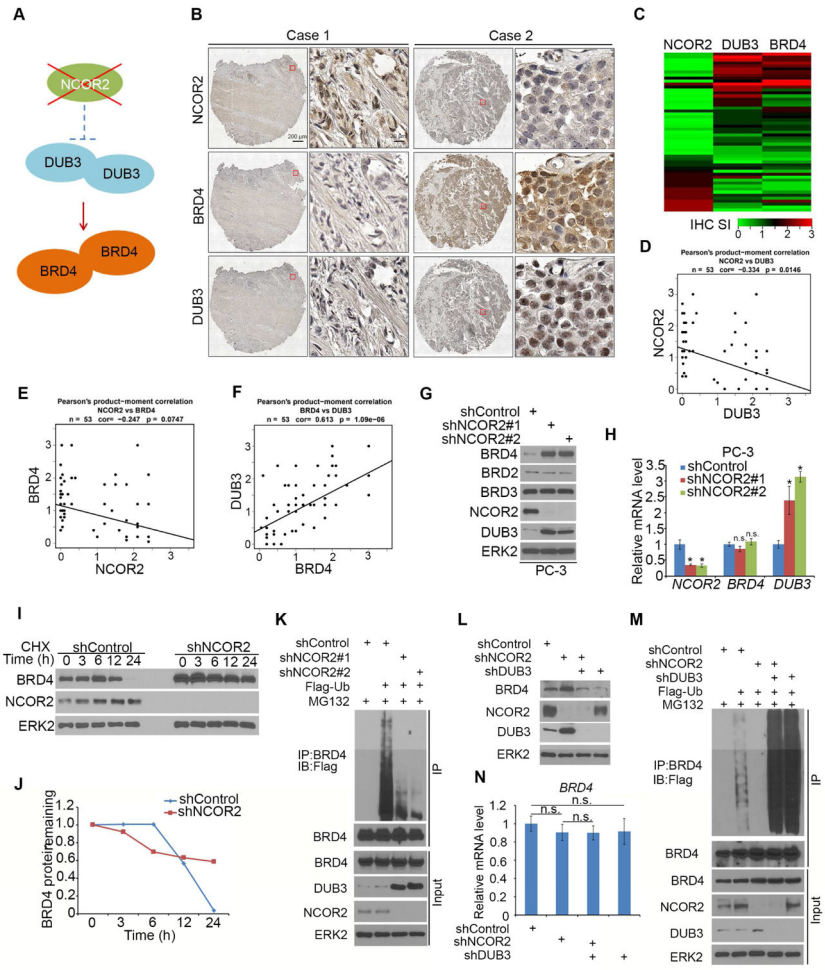

Figure 5. Decreased NCOR2 expression correlates with increased expression of DUB3 and BRD4 in prostate cancer cells and patient specimens

(A), a hypothetical model depicting that loss of NCOR2 correlates with increased expression of DUB3 and BRD4.

(B), representative images of IHC for NCOR2, DUB3, BRD4 proteins on TMA (n = 53) of prostate cancer specimens. Scale bars are indicated.

(C), heatmap showing the staining index (SI) of NCOR2, DUB3 and BRD4 proteins in TMA.

(D), correlation analysis of the SI of NCOR2 and DUB3 proteins in TMA.

(E), correlation analysis of the SI of NCOR2 and BRD4 proteins in TMA.

(F), correlation analysis of the SI of DUB3 and BRD4 proteins in TMA.

(G, H), PC-3 cells were infected with indicated shRNAs for48 h for Western blot (G) and RT-qPCR (H). * $P < 0.05$. n.s., not significant.

(I, J), PC-3 cells were infected with indicated shRNAs for 48 h followed by treatment of 50 μg/μl CHX for Western blot. Protein bands were quantified as in Figure 3E.

(K), PC-3 cells were infected with indicated shRNAs for 24 h followed by transfection with indicated plasmids for another 24 h. Cells were treated with MG132 for 8 h before immunoprecipitation and Western blot.
(L), PC-3 cells were infected with indicated shRNAs for 48 h for Western blot.
(M), PC-3 cells were infected with indicated shRNAs for 24 h followed by transfection with indicated plasmids for another 24 h. Cells were treated with MG132 for 8 h before immunoprecipitation and Western blot.
(N), PC-3 cells were infected as in (L) and harvested for RT-qPCR. Data are shown as mean ± SD (n=3). n.s., not significant.

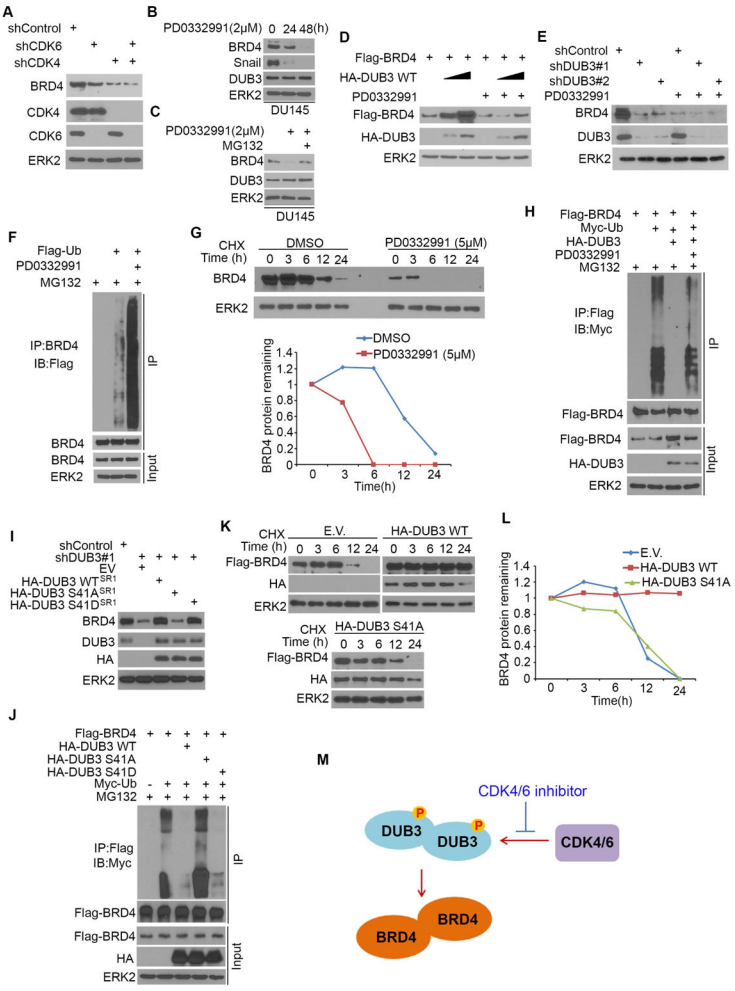

Figure 6. CDK4/6 inhibitor suppresses the deubiquitinase activity of DUB3 and promotes BRD4 degradation in prostate cancer cells

(A), DU145 cells were infected with indicated shRNA for 48 h for Western blot analysis.

(B), Western blot analysis in DU145 cells treated with 2 μM of PD0332991.

(C), Western blot analysis in DU145 cells treated with indicated inhibitors for 24 h.

(D), DU145 cells were transfected with indicated plasmids for 24 h followed by treatment with 2 μM of PD0332991 for another 24 h before Western blot.

(E), DU145 cells were infected with indicated shRNAs for 24 h and then treated with 2 μM of PD0332991 for another 24 h before Western blot.

(F), DU145 cells were transfected indicated plasmids and treated with 2 μM of PD0332991 for 24 h. Cells were treated with MG132 for 8 h before analysis.

(G), DU145 cells were treated with 5 μM of PD0332991 for 24 h followed by treatment with 50 μg/μl CHX. Protein bands were quantified as in Figure 3E.

(H), DU145 cells were transfected indicated plasmids and treated with 2 μM of PD0332991 for 24 h. Cells were treated with MG132 for 8 h before analysis.

(I), DU145 cells were infected with indicated shRNAs for 24 h followed by transfection of indicated constructs for another 24 h before analysis.

(J), DU145 cells were transfected indicated plasmids for 24 h and treated with MG132 for 8 h before harvested for immunoprecipitation and western blot analysis.
(K, L), DU145 cells were transfected with indicated plasmids for 24 h followed by treatment of 50 μg/μl CHX for Western blot. Protein bands were quantified as in (G).
(M), a hypothetical model depicting that CDK4/6 inhibitor suppresses the deubiquitinase activity of DUB3 and enhances BRD4 degradation.

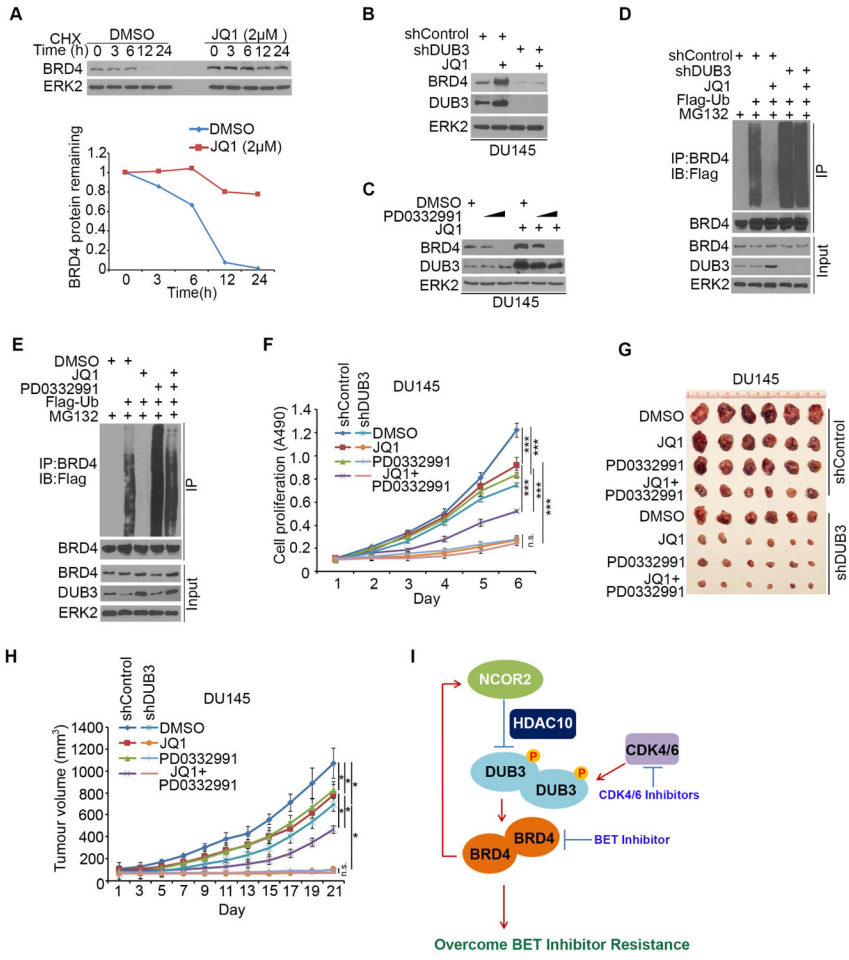

Figure 7. DUB3 inhibition by CDK4/6 inhibitor sensitizes prostate cancer cells to BET-inhibitor in vitro and in vivo

(A), DU145 cells were treated with JQ1 for 24 h followed by treatment of 50 μg/μl CHX for Western blot. Protein bands were quantified as in Figure 3E.

(B), DU145 cells were infected with indicated shRNAs for 24 h and treated with 2 μM of JQ1 for another 24 h before Western blot.

(C), Western blot analysis in DU145 cells 24 h after treated with indicated chemicals.

(D), DU145 cells were transfected indicated plasmids for 48 h and treated with MG132 for 8 h before analysis.

(E), DU145 cells were treated with indicated chemicals for 24 h and treated with MG132 for 8 h before analysis.

(F), DU145 cells were infected with indicated shRNAs for 48 h and treated with JQ1 (2 μM), PD0332991 (5 μM) or both before MTS assay. Data are shown as mean ± SD (n=6). *** $P < 0.001$, n.s., not significant.

(G, H), DU145 cells were infected with lentivirus as in (F) and injected s.c. into the right flank of NSG mice and treated with JQ1, PD0332991 or both. Tumor growth was measured every other day for 21 days. Tumors in each group at day 21 were harvested, photographed and shown in (G). Data in (H) are shown as mean ± SD (n = 6). * $P < 0.05$ comparing size of tumors in different groups at day 21.

(I), a hypothetical model depicting that DUB3 inhibition by CDK4/6 inhibitor sensitizes prostate cancer cells to BET-inhibitor.